ORIGINAL ARTICLE

John F. DiJoseph · Andrew Popplewell · Simon Tickle
Heather Ladyman · Alastair Lawson · Arthur Kunz
Kiran Khandke · Douglas C. Armellino
Erwin R. Boghaert · Philip R. Hamann
Karen Zinkewich-Peotti · Sue Stephens · Neil Weir
Nitin K. Damle

Antibody-targeted chemotherapy of B-cell lymphoma using calicheamicin conjugated to murine or humanized antibody against CD22

Abstract Antibody-targeted chemotherapy with immunoconjugates of calicheamicin is a clinically validated strategy in cancer therapy. This study describes the selection of a murine anti-CD22 mAb, m5/44, as a targeting agent, its conjugation to a derivative of calicheamicin (CalichDM) via either acid-labile or acid-stable linkers, the antitumor activity of CalichDM conjugated to m5/44, and its subsequent humanization by CDR grafting. Murine IgG1 mAb m5/44 was selected based on its subnanomolar affinity for CD22 and ability to be internalized into B cells. CalichDM conjugated to m5/44 caused potent growth inhibition of CD22$^+$ human B-cell lymphomas (BCLs) in vitro. The conjugate of m5/44 with an acid-labile linker was more potent than an acid-stable conjugate, a nonbinding conjugate with a similar acid-labile linker, or unconjugated CalichDMH in inhibiting BCL growth. CalichDM conjugated to m5/44 caused regression of established BCL xenografts in nude mice. In contrast, both unconjugated m5/44 and a nonbinding conjugate were ineffective against these xenografts. Based on the potent antitumor activity of m5/44-CalichDM conjugates, m5/44 was humanized by CDR grafting to create g5/44, an IgG4 anti-CD22 antibody. Both m5/44 and g5/44 bound CD22 with subnanomolar affinity. Competitive blocking with previously characterized murine anti-CD22 mAbs suggested that g5/44 recognizes epitope A located within the first N-terminal Ig-like domain of human CD22. Antitumor efficacy of CalichDM conjugated to g5/44 against BCL xenografts was more potent than its murine counterpart. Based on these results, a calicheamicin conjugate of g5/44, CMC-544, was selected for further development as a targeted chemotherapeutic agent for the treatment of B-cell malignancies.

Keywords B-lymphoid malignancies · CD22 · Cell surface molecules · Cytotoxic immunoconjugates · Humanized antibody · Targeted chemotherapy

Abbreviations

AcBut	4-(4′-Acetylphenoxy) butanoic acid
AcPAc	(3-Acetylphenyl) acetic acid
ATC	Antibody-targeted chemotherapy
BCL	B-cell lymphoma
CalichDM	N-Acetyl-γ-calicheamicin dimethyl disulfide derivative(s)
CalichDMA	CalichDM acid
CalichDMH	CalichDM hydrazide
CDR	Complementarity determining region
NHL	Non-Hodgkin's lymphoma
PBMC	Peripheral blood mononuclear cell
TAA	Tumor-associated antigen

J. F. DiJoseph · K. Khandke · D. C. Armellino
E. R. Boghaert · N. K. Damle (✉)
Oncology Discovery, Wyeth Research,
200/4604, 401 North Middletown Road,
Pearl River, NY 10965, USA
E-mail: damlen@wyeth.com
Tel.: +1- 845-6023984
Fax: +1-845-6025557

A. Kunz · P. R. Hamann
Chemical Sciences, Wyeth Research, Pearl River,
New York, USA

A. Popplewell · S. Tickle · H. Ladyman · A. Lawson
K. Zinkewich-Peotti · S. Stephens · N. Weir
Celltech R&D, Slough, UK

Introduction

Monoclonal antibodies (mAbs) targeted to tumor-associated antigens (TAAs) have been widely used in various experimental therapeutic approaches that include the

12

specific delivery of radioactive isotopes in the form of radioimmunotherapeutics, or of cytotoxic agents in the form of antibody-drug conjugates [1]. Antibodies or their fragments have been either chemically linked or genetically fused to xenotoxins to produce immunotoxins. In addition, anti-TAA mAb(s), chemically conjugated or genetically fused to enzymes, have been used to evaluate antibody-directed enzyme prodrug therapy [2]. Antibody-targeted chemotherapy (ATC) is now an accepted therapeutic strategy in which a cytotoxic agent is conjugated to an anti-TAA mAb that specifically binds to the TAA on the surface of tumor cells and is internalized, resulting in its intracellular delivery [3]. This strategy facilitates preferential delivery of the cytotoxic agent into the tumor cells and reduces nonspecific toxicity in normal tissues.

The ATC strategy was validated with the approval of gemtuzumab ozogamicin (Mylotarg or CMA-676) by the US FDA in May 2000 [4]. Gemtuzumab ozogamicin is a CD33-targeted immunoconjugate in which a humanized anti-CD33 mAb, hP67.6, is conjugated via an acid-labile AcBut hybrid linker to N-acetyl γ-calicheamicin dimethyl hydrazide (CalichDMH), a derivative of a potent cytotoxic agent, γ-calicheamicin [5–9]. Calicheamicin-γ binds DNA in the minor groove and undergoes thiol-dependent structural changes in its enediyne moiety to generate a di-radical that abstracts hydrogens from the phosphodiester backbone of DNA causing double-strand DNA breaks leading to cell death [10–12]. Gemtuzumab ozogamicin is approved for the treatment of acute myeloid leukemia (AML) in elderly ($\geq$60 years of age) patients in first relapse who are not candidates for other therapies [13].

The ATC strategy could be similarly applied to B-lymphoid malignancies using an immunoconjugate of N-acetyl γ-calicheamicin dimethyl disulfides (CalichDM) targeted to B-cell lineage–specific differentiation antigens. CD22 is a 130-kDa type 1 transmembrane glycoprotein that is selectively displayed on the surface of most mature B lymphocytes and their malignant counterparts [14]. It is not expressed on the surface of non-B lineages including hematopoietic stem cells and pre-B cells [15]. Similar to CD33, CD22 is a sialic acid–binding lectin (Siglec-2) and a member of the Ig superfamily [16, 17]. Its N-terminal IgV-like domain recognizes α-2,6-linked terminal sialic acid residues on glycoproteins on the surface of cells that interact with B cells and regulates activation of B cells [15–17]. Antibodies bound to CD22 are rapidly internalized [18, 19] making CD22 ideally suited for targeted delivery of cytotoxic agents [20–22]. Using a murine anti-CD22 mAb, m5/44, as a CD22-targeting agent, the present study demonstrates potent antitumor activity of m5/44 conjugated to CalichDM. It further describes humanization of m5/44 by CDR grafting to generate g5/44, a humanized IgG4 anti-CD22 mAb used to create a CD22-targeted conjugate of CalichDMH. This conjugate of CalichDMH, like its murine counterpart, causes regression of established BCL xenografts in nude mice.

Materials and methods

Cell lines

B-cell lymphoma (BCL) lines Daudi (CCL-213), Raji (CCL-86), Ramos (CRL-1923), and RL (CRL-2261), and myeloid leukemia cell line HL-60 (CCL-240) were all obtained from the American Type Culture Collection (ATCC, Manassas, Va., USA). The cell lines were determined to be mycoplasma free as determined by a polymerase chain reaction mycoplasma detection assay (ATCC). The cell lines were maintained in RPMI 1640 medium supplemented with 10% fetal bovine serum (FBS), 10 mM HEPES, 1 mM sodium pyruvate, 0.2% glucose, penicillin G sodium 100 U/ml, and streptomycin sulfate 100 μg/ml.

Mice

Female, BALB/c nu/nu (nude) mice (18–23 g) were obtained from Charles River Laboratories, Wilmington, Mass., USA and BALB/c mice from Harlan Laboratories, UK. All mice were provided with food and water ad libitum throughout the studies. All experimental procedures involving mice were approved by the Celltech Ethical Review Committee and Wyeth Animal Care and Use Committee according to established guidelines.

Monoclonal antibodies and CD22 antigen

A number of purified murine anti-CD22 mAbs were obtained from their respective vendors: HD239, MYG13, RFB-4, SJ10.1H11 (Santa Cruz Biotech, Santa Cruz, Calif., USA); S-HCL1/anti-Leu 14 (Becton Dickinson, Franklin Lakes, N.J., USA), 4KB128 and To15 (Dako Corp, Carpinteria, Calif., USA). In addition, a panel of murine mAbs to human CD22 was developed using conventional hybridoma technology [23] and screened for isotype, cell binding, internalization on Daudi cells and on peripheral blood B cells, and binding affinity to human CD22-mFc antigen. A human CD22-mFc construct encoding the entire extracellular domain of human CD22 genetically fused to the Fc portion of murine IgG1 was prepared and expressed in NS0 cells. The humanized IgG4 anti-CD33 mAb, hP67.6, and its conjugate of CalichDMH, gemtuzumab ozogamicin (Mylotarg or CMA-676), have been described previously [5, 9].

Cloning of m5/44 V-region genes

Total RNA was prepared from m5/44 hybridoma cells using the RNeasy kit (Qiagen, Valencia, Calif., USA). RNA was reverse transcribed to cDNA using the Clontech (Palo Alto, Calif., USA) cDNA Advantage

reverse transcriptase for polymerase chain reaction (PCR) kit. This cDNA was then used as the template for PCR using a set of ''forward'' degenerate primers designed to anneal to DNA encoding the conserved signal sequence, and a reverse primer annealing to DNA encoding the framework 4/constant region junction. PCR was performed using AmpliTaq enzyme and buffer (Applied Biosystems, Foster City, Calif., USA). The resultant PCR products were cloned into sequencing vectors (InVitrogen TOPO-TA cloning kit; InVitrogen, Carlsbad, Calif., USA), and the DNA sequence was determined. N-Terminal protein sequencing of the purified antibody (from hybridoma) was used to confirm that the translated sequences corresponded to the observed protein sequence (data not shown).

Plasmid construction and expression of chimeric constructs

The murine V-region sequences were cloned into the expression vectors pMR10.1 and pMR14 [24]. These are vectors designed for the expression of light and heavy chain, respectively, containing DNA encoding constant regions of human κ light chain and human γ-4 heavy chain. The VL DNA was subcloned into the light chain expression vector, creating plasmid pMR10 (544 cL). The VH DNA was subcloned into the heavy chain expression vector, creating plasmid pMR14 (544 cH). Transient cotransfection of both expression vectors into CHO-L761 cells generated chimeric c5/44 antibody. Transfections were carried out using Lipofectamine reagent according to manufacturer's instructions (InVitrogen, Carlsbad, Calif., USA). Mutations to CDR-H2 were carried out by a PCR approach, using oligonucleotides with specific mismatched bases to introduce desired codon changes.

Modulation of anti-CD22 mAb bound to B cells

Peripheral blood mononuclear cells (PBMCs; isolated from human blood) or BCL and anti-CD22 mAb were mixed (0.5 μg of mAb/5×10^5 cells/ml) and incubated on ice for 60 min after which cells were washed. The antibody-treated cell suspensions were then transferred to a 37°C water bath for timed intervals between 0 and 24 h. At the defined times, tubes with cells were immediately returned to iced (4°C) water. Tubes were centrifuged and the supernatant removed to quantify the presence of murine IgG by ELISA in order to confirm that the antibody bound to the cell surface was not shed in the surrounding medium. R-Phycoerythrin-conjugated donkey antimouse IgG (H + L chains) antibody (Jackson Immunoresearch Laboratories, West Grove, Pa., USA) was added to the cell pellet, and samples were maintained in iced water for 1 h then washed as above. Cells were then resuspended in wash buffer and analyzed by flow cytometry to detect the antibody bound to the cells.

Conjugation of anti-CD22 mAb with calicheamicin

The murine anti-CD22 mAb m5/44 was covalently conjugated on the ε-NH_2 groups of lysines to either CalichDMH with the acid-labile AcPAc ((3-acetylphenyl)acetic acid) linker or to N-acetyl γ-calicheamicin dimethyl acid (CalichDMA) with the acid-stable Amide linker [25]. The humanized version of m5/44, g5/44, was conjugated to CalichDMH with the acid-labile AcBut (4-(4′-acetylphenoxy) butanoic acid) linker [9]. Attempts to conjugate m5/44 with CalichDMH using the AcBut linker resulted in aggregated conjugates and thus were not evaluated. After the conjugation reaction, conjugated monomeric IgG antibody was separated from the aggregated conjugated antibody by gel permeation chromatography. Only the monomeric IgG conjugates as defined by the size-exclusion profile of the antibody conjugates were used in various investigations. The AcPAc-linked conjugates of m5/44 had an average calicheamicin loading of 18 μg of CalichDMH per milligram of the antibody protein (1.6 M/M). The average drug loading of the Amide-linked calicheamicin conjugates was 20 μg of CalichDMA per milligram of antibody (1.8 M/M). CMA-676 is comprised of humanized IgG4 anti-CD33 mAb, hP67.6, which is linked to CalichDMH via the AcBut linker with an average drug loading of 35 μg of CalichDMH per milligram of hP67.6 protein (3.2 M/M). All conjugates were confirmed as having low endotoxin (< 5.0 EU/ml) as determined by the Limulus amebocyte lysate test (BioWhittaker, Walkersville, Md., USA).

Cytotoxicity assays

Ramos and Raji BCL and HL-60 myeloid leukemic cell lines were cultured in the presence of various concentrations of unconjugated calicheamicin (CalichDMH), unconjugated anti-CD22 mAb m5/44, NAc-γ-calicheamicin derivatives conjugated to m5/44, or CMA-676. Calicheamicin conjugate concentrations were based on the content of calicheamicin equivalents. Concentrations of unconjugated mAb were based on protein content. Ninety-six-hour cell viability was measured by propidium iodide (PI) exclusion and analyzed by flow cytometry (FACSort, Becton Dickinson Immunocytometry System; Becton Dickinson, San Jose, Calif., USA). The region for viable cells was set using both the forward light scatter and red fluorescence properties of the cells. Nonviable cells lose their membrane integrity, shrink in size, and allow diffusion of PI in the nucleus to bind cellular DNA resulting in lower forward light scatter and increased red fluorescence. The loss of viability was determined by the loss of cells from within the gated region defining viable cells [26]. The average number of viable cells per six replicate cultures was calculated. The percentage survival of BCL cells in these cultures was calculated using the following equation: percentage survival = 100×(number of viable cells in treated cul-

14

tures) / (number of viable cells in control cultures). IC$_{50}$s (with 95% confidence intervals) were calculated by logistic nonlinear regression and are reported as the calicheamicin concentration from each treatment group that causes 50% loss of cell viability.

Humanization of m5/44 into g5/44

The methodology described by Adair et al. [27] was used to design CDR-grafted variants using selected human acceptor frameworks. Genes were designed to encode the grafted sequences gHa and gLa, and a series of overlapping oligonucleotides were designed and constructed. A PCR assembly technique was employed to construct the CDR-grafted V-region genes from these oligonucleotides [28]. The grafted variants gLb and gHb-d were constructed from the parental grafts gLa and gHa by PCR mutagenesis, using oligonucleotides with specific mismatched bases to introduce desired codon changes (see below).

Competition of CD22 binding among murine and humanized mAb

Murine antibody m5/44 (final concentration of 600 ng/ml) was added to humanized, grafted antibodies (in the range of 0.015–1.5 µg/ml) in a 96-well plate. Ramos cells (1.5×10^5) were added to the wells, and the plate was incubated on ice for 1 h. Control wells contained 1.5 µg/ml of either humanized grafted antibody or m5/44. The cells were washed twice with wash buffer (PBS + 5% FBS) after which secondary antibody, either RPE-conjugated donkey antimouse IgG (H + L chains) (Jackson Immunoresearch Laboratories, West Grove, Pa., USA) or FITC-conjugated goat-antimouse IgG (H + L chains) (Zymed, South San Francisco, Calif., USA), was added and incubated on ice for 1 h. Cells were then washed with wash buffer and analyzed by flow cytometry.

Biosensor analysis

Biosensor analysis was carried out using a BIAcore 2000 (BIAcore AB, Uppsala, Sweden). CD22-mFc was covalently immobilized on the N-hydroxysuccinimide–activated carboxymethyl dextran-coated biosensor chip (CM5) using a standard amine-coupling chemistry at a protein density of approximately 2,000 resonance units. Samples of antibodies or their calicheamicin conjugates were diluted in the HBS buffer (10 mM HEPES, pH 7.4, containing 150 mM NaCl, 3 mM EDTA, and 0.005% polysorbate 20 [v/v]) and injected in the concentration range of 1–100 nM over the CD22-mFc-coated biosensor chip surface at a flow rate of 30 µl/min for 3 min to allow for binding. Dissociation of the bound antibody was monitored after washing the biosensor chip with the HBS buffer for 15 min. The antigenic surface was regenerated by washing the biosensor chip with 15 µl of the regeneration buffer (10 mM NaOH and 200 mM NaCl) for 30 s, followed by a stabilization time of 2 min before the next cycle. Kinetic constants were calculated by nonlinear least-square regression analysis using a 1:1 Langmuir binding curve fitting model and BIAevaluation program (version 3.0; BIAcore).

Subcutaneous BCL xenografts

Female, athymic nude mice were exposed to total body irradiation (400 rad) to further suppress their residual immune system and facilitate the establishment of BCL xenografts. Three days later, irradiated mice were injected s.c. with 1×10^7 Ramos or Raji cells suspended in Matrigel (Collaborative Biomedical Products, Belford, Mass., USA) diluted 1:1 in RPMI 1640 medium, in the dorsal, right flank. When the tumors reached a mass of 0.3–0.6 g, they were staged to ensure uniformity of the tumor mass (n = 7 to 9 mice/group) prior to the administration of therapy. Conjugated CalichDM derivatives, unconjugated antibody (m5/44), or CMA-676 were administered i.p. in sterile saline (0.2 ml/mouse) on day 1 and the same treatment was repeated twice, 4 days apart (Q4D×3). Doses of conjugated CalichDM were based on the quantity of calicheamicin equivalents. Length and width (in cm) of the tumors were measured at least once a week and their mass was calculated as tumor mass (g) = 0.5×(tumor width^2)(tumor length). Mean (± SEM) tumor mass for each treatment group was calculated and compared to the vehicle-treated group for statistical significance using a one-sided t-test analysis of variance and subsequent pairwise comparisons to vehicle with the error term for the t-test based on the pooled variance across all treatment groups. Tumor mass values for each treatment group were recorded up to 50 days after the initiation of treatment or until either tumor-bearing mice died or the tumors grew to 15% of the body weight, at which time these mice were humanely euthanized according to institutional regulations. The number of tumor-free mice at the end of each study for each treatment group was also recorded.

Results

Modulation of anti-CD22 mAb bound to B lymphoma cells

A panel of 17 murine mAbs was made against human CD22. Three antibodies from this panel (m5/44, m6/13, and m38) were selected for further evaluation based on their subnanomolar affinity for CD22-mFc (K$_D$ = 60–500 pM), and their ability to bind and modulate CD22 on the surface of Daudi BCL and PBMC cells (Fig. 1a, b). The modulation of surface-bound mAb as defined by the loss of surface display of the bound mAb was evaluated by flow cytometry.
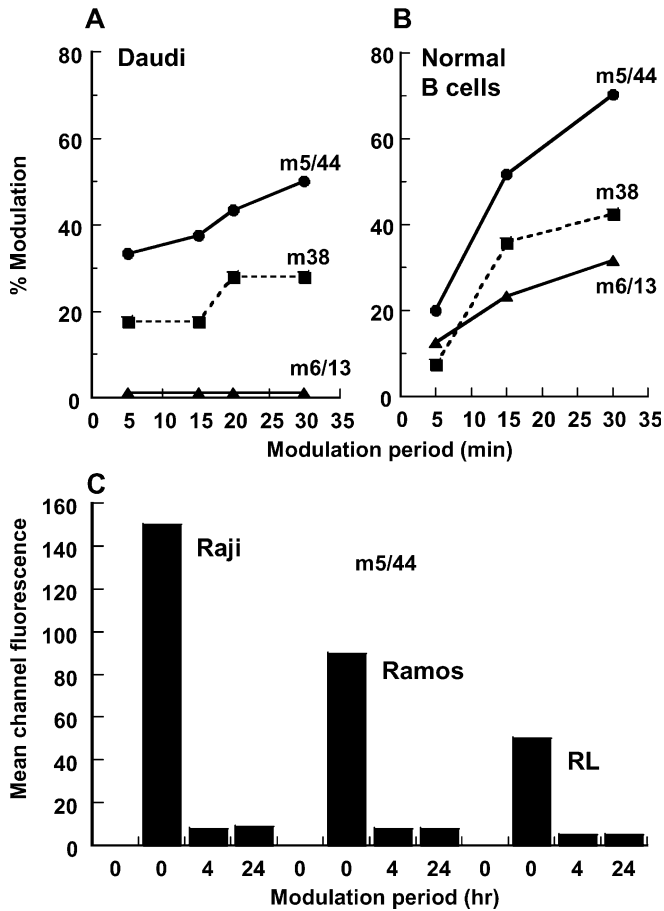
Fig. 1a–c Modulation of mAbs bound to CD22 expressed on the surface of normal peripheral blood–derived B cells and BCLs. Anti-CD22 mAbs were allowed to bind at 4°C to either Daudi BCLs (a) or normal peripheral blood B cells (b), and washed to remove unbound mAb. The B cells were further maintained at 37°C for varying lengths of time up to 30 min after which the surface retention of the anti-CD22 mAb was assessed by indirect immunofluorescence analysis. A similar evaluation was conducted using three distinct BCLs (c), except that the modulation period was extended to 24 h

Shedding of mAbs from the cell surface as assessed by ELISA was shown to be below the limit of detection, consistent with their high-affinity binding to CD22. While each of the three mAbs bound similarly to CD22 on B cells (data not shown), mAb m5/44 demonstrated the maximum modulation, with 50% of the initial surface-bound m5/44 no longer detectable after 30 min. In contrast, mAb m6/13 bound to, but failed to modulate from, the Daudi BCL surface (Fig. 1a). Similar rank order of modulation (m5/44 > m38 > m6/13) was observed using PBMC (Fig. 1b). The modulation of the cell surface–bound m5/44 was further confirmed using CD22$^+$ Ramos, Raji, and RL BCLs (Fig. 1c). Each of these BCLs showed > 90% modulation of the bound m5/44 over the 4-h period. Examination of these cells after 24 h failed to demonstrate any membrane reappearance of

m5/44. These observations suggest that m5/44, bound to the surface CD22, is rapidly and almost completely (> 90%) modulated without recycling over the 24-h period. The lack of any detectable antibody in the culture supernatants, combined with the rapid modulation of the bound mAb, is indicative of the internalization of the mAb bound to the cell surface CD22. Based on its ability to bind human CD22 with high affinity ($K_D = 200$ pM) and internalize (modulation without shedding) in BCLs, m5/44 was selected for further investigations.

Calicheamicin conjugation of m5/44

Three linkers were used to covalently conjugate CalichDM derivatives to mAbs and the chemical structures of these are shown in Fig. 2. CalichDMH can be conjugated to mAb using the AcBut or AcPAc linker. The AcBut linker is the preferred linker based on our experience with the currently marketed agent, gemtuzumab ozogamicin (Mylotarg, CMA-676). Both the AcBut- and the AcPAc-linked conjugates include an acid-labile hydrazone functional group that undergoes hydrolysis at similar rates under acidic conditions, releasing CalichDMH from its covalently conjugated state [9]. Unlike the conjugation of humanized mAb to CalichDMH via the AcBut linker, similar conjugation of murine mAb resulted in significant aggregation, rendering the murine mAb conjugates unusable. This problem was avoided by the use of the AcPAc linker that allowed the generation of conjugates from which CalichDMH can be released under acidic conditions. Thus, m5/44 was conjugated to CalichDMH using the acid-labile AcPAc linker and to CalichDMA using the acid-stable Amide linker. CMA-676, an AcBut-linked conjugate of humanized anti-CD33 mAb, was used as a nonbinding negative control conjugate in experiments using CD22$^+$CD33$^-$ BCLs.

In vitro cytotoxic activity of calicheamicin conjugated to anti-CD22 mAb

The effect of m5/44, conjugated to CalichDM with the AcPAc and the Amide linkers, on the growth of CD22$^+$CD33$^-$ Raji and Ramos BCLs was examined in vitro. CalichDMH, unconjugated m5/44, and CMA-676 were used as controls. As shown in Table 1, both conjugates of m5/44 inhibited the growth of Ramos and Raji BCLs. The AcPAc-linked conjugate of m5/44 was 4-fold to 8-fold more potent than the Amide-linked conjugate of the same mAb. The cytotoxic potency of the amide-linked conjugate of m5/44 and unconjugated CalichDMH was similar. Unconjugated m5/44 had no effect on the growth of either BCL at concentrations up to 100 μg/ml, demonstrating that the potent growth-inhibitory effect of CD22-targeted conjugates was due to the cytotoxic activity of CalichDM. CD33-targeted CMA-676, in spite of the presence of the acid-labile

Fig. 2 Structural representation of the linkers used to conjugate CalichDM derivatives to the targeting mAb. Both the AcBut- and AcPAc-linked conjugates include an acid-labile hydrazone functionality. The amide-linked conjugate lacks such an acid-labile group
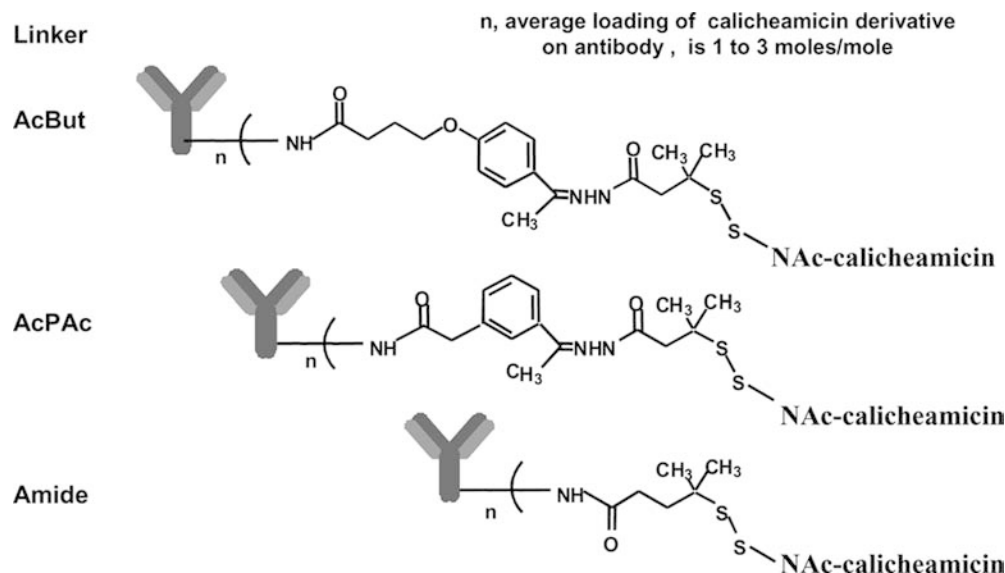
AcBut linker, was 20- to 260-fold less potent in inhibiting BCL growth than the CD22-targeted AcPAc-linked conjugate of m5/44. In contrast, CMA-676 was 166-fold more potent than the CD22-targeted conjugate with acid-labile linker in inhibiting the growth of $CD22^-CD33^+$ HL-60 myeloid leukemic cells. These results demonstrate that CD22-targeted delivery of CalichDM can produce a potent and specific cytotoxic activity against $CD22^+$ BCLs.

Antitumor efficacy of CD22-targeted calicheamicin immunoconjugate against B-lymphoma xenografts

CalichDM conjugates of m5/44 were examined for their antitumor efficacy against s.c. Ramos or Raji BCL xenografts established in nude mice. Conjugates of CalichDM derivatives were administered i.p. as three doses injected 4 days apart (Q4D×3) [25] in BCL xenograft-bearing mice. The antitumor activity of CalichDM conjugates against Ramos BCL xenografts and Raji BCL xenografts are shown in Figs. 3 and 4, respectively. CalichDM conjugated to m5/44 via either the AcPAc or

the Amide linker at a dose of 160 μg/kg of conjugated CalichDM inhibited BCL growth in both models. This dose of conjugated CalichDM has been shown to be lower than its maximum nonlethal dose and optimal for its antitumor activity [25]. In contrast, the nonbinding conjugate, CMA-676, and m5/44 (administered at a dose of 8 mg/kg equivalent to the antibody quantity in its calicheamicin conjugates) were ineffective against the BCL xenografts. After confirming the ability of m5/44 to target and deliver CalichDM to BCLs and cause potent anti-BCL activity, m5/44 was humanized to create g5/44 for further evaluation as a CD22-targeted drug-delivery agent.

Cloning and expression of chimeric 5/44 antibodies

A PCR approach was used to clone the V-region genes from hybridoma m5/44, and the DNA sequence was determined and translated to reveal the protein sequence (Fig. 5). Vectors expressing a chimeric version of this antibody, with the mouse V-regions and human constant regions (κ light chain, γ-4 heavy chain) were

Table 1 Cytotoxic activity of calicheamicin conjugates against human BCLs in vitro. Human B lymphoma cells were cultured for 96 h in the presence of various concentrations of CalichDM derivatives conjugated to m5/44 with either the Amide linker or the AcPAc linker, CD33-targeted CMA-676, or CalichDMH, after which the viable cell number in each culture was enumerated by their exclusion of PI and detected by flow cytometry. Concentrations of the conjugates of CalichDM derivatives were based on the calicheamicin equivalents (nM) and the unconjugated mAb m5/44 was used based on its protein concentration
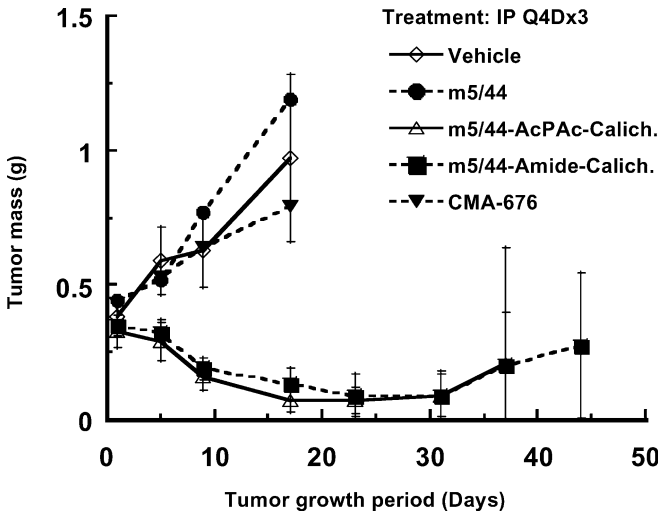
Treatment	IC_{50} (nM of calicheamicin equivalents)		
	$CD22^+CD33^-$ Raji	$CD22^+CD33^-$ Ramos	$CD22^-CD33^+$ HL60
Anti-CD22 mAb m5/44 unconjugated	> 100 μg/ml	> 100 μg/ml	Not determined
CalichDMH	0.41	0.055	0.5
Anti-CD22 m5/44-amide-CalichDMA	0.34	0.041	> 67.6
Anti-CD22 m5/44-AcPAc-CalichDMH	0.08	0.005	7.5
Anti-CD33 hP67.6-AcBut-CalichDMH (CMA-676)	1.63	1.285	0.045

Fig. 3A–C Effect of CalichDM conjugated to m5/44 on the growth of Ramos BCL xenografts. Subcutaneous tumors were established prior to the administration of CalichDM conjugates at a fixed dose of 160 µg of conjugated CalichDM/kg. Three such doses were administered 4 days apart (Q4D×3). CD33-targeted conjugate of CalichDMH (CMA-676) was used as a nonspecific conjugate. Unconjugated m5/44 at 8 mg/kg was used as a control. Three separate studies are presented in panels **A**, **B**, and **C**. Results are presented as mean tumor mass ± SEM
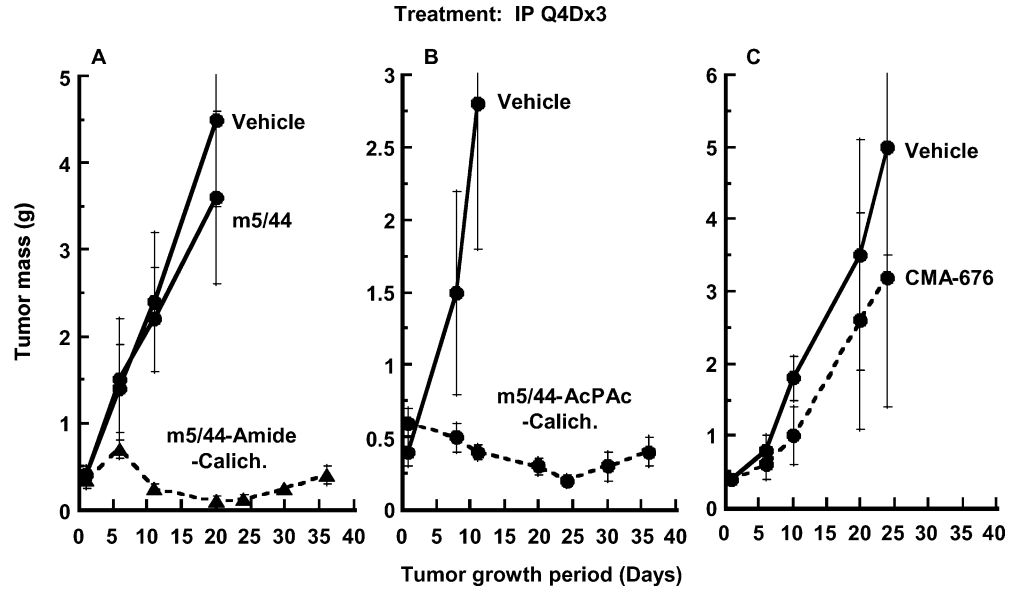
assembled. The m5/44 VH sequence (Fig. 5a) revealed a potential N-linked glycosylation site in CDR-H2 (residue N55). In addition, a lysine residue within CDR-H2 (K60), a potential site for calicheamicin conjugation, was of concern, since calicheamicin conjugation close to the antigen-binding site might be expected to interfere with its binding to CD22. The following constructs were made to assess the effect of removal of these residues: cH-N55Q, cH-T57A, and cH-K60R. The N55Q and T57A changes ablate the glycosylation site by changing the amino acid sequence away from the consensus N-X-T/S; the K60R mutation replaces the potentially reactive

Fig. 4 Effect of CalichDM conjugated to m5/44 on the growth of Raji BCL xenografts. Subcutaneous tumors were established to an average mass of 300 mg after which CalichDM conjugates of m5/44 were administered at 160 µg of conjugated CalichDM/kg. Three such doses were administered 4 days apart (Q4D×3). The CD33-targeted conjugate of CalichDMH (CMA-676) was used as a nonspecific conjugate. Unconjugated m5/44 at 8 mg/kg was used as a control. Results are presented as mean tumor mass ± SEM

lysine with the similarly positively charged residue arginine. The resultant cH variant plasmids were cotransfected with the cL plasmid to generate expressed chimeric antibody variants. They were then analyzed for binding affinity to CD22-mFc protein using a BIAcore assay (Table 2). Removal of the glycosylation site in construct T57A resulted in a 2- to 3-fold faster on-rate and a significantly slower off-rate compared with the chimeric, giving an overall improvement in affinity of approximately 3- to 5-fold. The N55Q mutation had no effect on affinity. This result was unexpected since removal of any carbohydrate alone (the N55Q change) apparently had no effect on its binding to CD22, therefore the improved affinity requires the specific T57A change. One possible explanation is that regardless of the presence of carbohydrate, the threonine at position 57 exerts a negative effect on binding that is removed on conversion to alanine. Replacement of lysine at position 60 with arginine (K60R) had no effect on affinity of the antibody, and this change removed a potential reactive site that might have negatively impacted the affinity of the antibody after its conjugation with calicheamicin. Both these mutations (T57A and K60R) were therefore retained in the CDR-H2 sequence of the humanized heavy chains.

Humanization strategy

Germline acceptor frameworks were selected from human VH subgroup I (VH1-3/DP-7) [29] and human VK subgroup I (O12/DPK9) [30]. For the heavy chain, the framework 4 acceptor sequence was derived from human J-region sequence JH-4; the human JK-1 sequence was used for the light chain framework 4. Figure 5 shows the protein sequences of the m5/44 heavy and light chains compared with the human acceptor frameworks, and also the designed grafted sequences. The

A) 5/44 Heavy Chain Sequence Alignment

```
                    10        20        30            40        50
VH      EVQLQQSGTVLARPGASVKMSCKAS GYRFTNYWIH WVKQRPGQGLEWIG GINP
        *    *    *****       *                 * *          *
DP-7    QVQLVQSGAEVKKPGASVKVSCKAS            WVRQAPGQGLEWMG
        *                                              *
gHa-d   EVQLVQSGAEVKKPGASVKVSCKAS GYRFTNYWIH WVRQAPGQGLEWIG GINP


                  60        70        80        90        100
VH      GNNYTTYKRNLKG KATLTAVTSASTAYMDLSSLTSEDSAVYYCTR EGYGNYG
                      ** * **  *  *    *     *     *     *
DP-7             KFQG RVTMTRDTSTSTVYMELSSLRSEDTAVYYCAR
                      * * *                         *
gHa     GNNYATYRRNLKG RATLTADTSTSTVYMELSSLRSEDTAVYYCTR EGYGNYG
gHb     GNNYATYRRNLKG RVTMTADTSTSTVYMELSSLRSEDTAVYYCTR EGYGNYG
gHc     GNNYATYRRKFQG RATLTADTSTSTVYMELSSLRSEDTAVYYCTR EGYGNYG
gHd     GNNYATYRRKFQG RVTMTADTSTSTVYMELSSLRSEDTAVYYCTR EGYGNYG


                  110
VH      AWFAY WGQGTLVTVSS

JH4           WGQGTLVTVSS

gHa-d   AWFAY WGQGTLVTVSS
```

B) Light Chain Sequence Alignment

```
                    10        20                    40
VL      DVVVTQTPLSLPVSFGDQVSISC RSSQSLANSYGNTFLS WYLHKPGQSPQLLIY
        ***   *  * **    * *                     **   ** *
DPK9    DIQMTQSPSSLSASVGDRVTITC                  WYQQKPGKAPKLLIY
        * *                                      **        *
gLa     DVQVTQSPSSLSASVGDRVTITC RSSQSLANSYGNTFLS WYLHKPGKAPQLLIY
gLb     DVVVTQSPSSLSASVGDRVTITC RSSQSLANSYGNTFLS WYLHKPGKAPQLLIY


                  60        70        80        90
VL      GISNRFS GVPDRFTGSGSGTDFTLKISTIKPEDLGMYYC LQGTHQPYT
                      *  *         *  ***    ***
DPK9            GVPSRFSGSGSGTDFTLTISSLQPEDFATYYC
                      *
gLa-b   GISNRFS GVPDRFSGSGSGTDFTLTISSLQPEDFATYYC LQGTHQPYT


                  100
VL      FGGGTKLEIKR
            *   *
JK1     FGQGTKVEIKR

gLa-b   FGQGTKVEIKR
```

CDRs are shown according to a combination of the sequence hypervariability definition [31] and the structural definition [32]. In practice, this means that the larger sequence-based limits apply to all CDRs except CDR-H1, which comprises residues H26–H35. The alignment shows that there are 22 framework differences between the donor and acceptor heavy chain frameworks. The light chain alignment shows that there are 27 framework differences between the donor and acceptor sequences. At each position of sequence difference, an analysis was made of the potential of the murine residue to contribute to antigen binding, either directly or indirectly through effects on packing or at the VH/VL

Table 2 Binding of chimeric 5/44 and its mutants to CD22. Human CD22-mFc fusion protein was captured on antimouse IgG Fc-specific antibody-coated biosensor chip. The binding of chimeric 5/44 and its three mutants to captured CD22-mFc was studied using BIAcore. The above mutations were localized in the CDR2 of the variable domain of the heavy chain of chimeric 5/44

Mutation in CDRH2	K_a ($\times 10^5$), 1/Ms	K_d ($\times 10^{-4}$), 1/s	K_D ($\times 10^{-10}$), M	$\sim K_D$, nM
Murine VH	2.9	1.1	3.9	0.4
N55Q	5.8	1.9	3.3	0.3
T57A	7.8	0.5	0.7	0.07
K60R	5.0	1.0	2.0	0.2
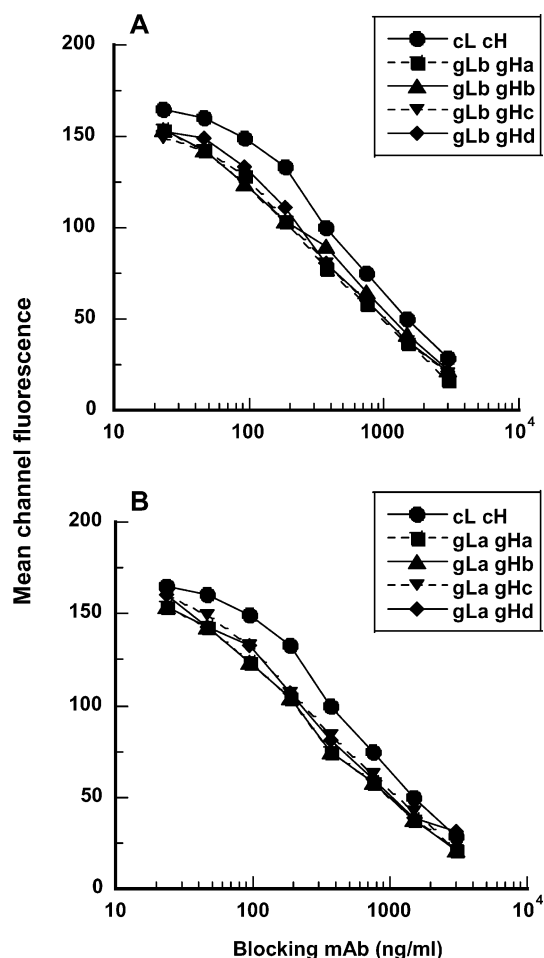
Fig. 6a,b Competitive inhibition of the binding of murine anti-CD22 mAb, m5/44, to Ramos BCL by its humanized versions assembled by combinations of four distinct grafts of heavy chain (gHa–d) and two distinct grafts of light chain (gLa, gLb). Increasing concentrations of the humanized mAb were mixed with the fixed concentration of m5/44 and then allowed to bind to Ramos BCL. Binding of the murine mAb, m5/44, was monitored by indirect immunofluorescence analysis using flow cytometry. The chimeric version of m5/44 (cL cH) was also used in this evaluation as a positive control

interface. If a murine residue was considered important and sufficiently different from the human in terms of size, polarity or charge, then that murine residue was back-mutated into the human acceptor sequence. In this way, four VH grafts and two VK grafts were designed, as shown in the Fig. 5. Grafts gHc and gHd contain three additional human residues at the C-terminal end of CDR-H2. This portion of the CDR is not at the antigen-binding surface, and so introduction of human residues can be tolerated.

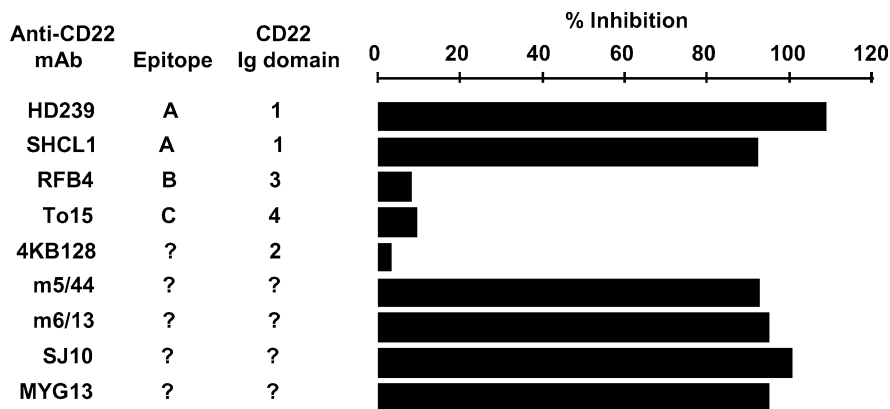Characterization of humanized variants of anti-CD22 mAb

The vectors encoding grafted variants were cotransfected into CHO cells in a variety of combinations, and the expressed humanized mAbs were compared with the chimeric 5/44 antibody. Binding activity was assessed in a competition assay, competing with the binding of the original m5/44 antibody to Ramos BCL (Fig. 6). The binding of each of the eight grafted variants to cell surface CD22 was indistinguishable from that of the others. This suggests that heavy chain residues A67 and L69, and light chain residue V3 are not important for antigen binding and can be replaced by the human residues. Each graft was found to perform more effectively than the chimeric antibody at competing against m5/44. Hence CD22-binding activity was not diminished by the CDR-grafting process, and was slightly improved. This modest improvement is most likely due to the T57A change present in each heavy chain graft. The introduction of the three additional human residues at the end of CDR-H2 (gHc and gHd) did not affect CD22 binding of the grafted mAb.

Since all the grafted variants were fully active, the graft combination of gLa-gHd with the least number of murine residues was selected for further studies. The light chain graft gLa has six donor framework residues. Residues V2, V4, L37, and Q45 are potentially important packing residues. Residue H38 is at the VH/VL interface. Residue D60 is a surface residue close to the CDR-L2 and may directly contribute to the antigen binding. The heavy chain graft gHd has four donor framework residues. Residues E1 and A71 are surface residues close to the CDRs. Residue I48 is a potential packing residue. Residue T93 is present at the VH/VL interface. Of these residues, E1 and A71 are found in other germline genes of human subgroup I. The selected humanized IgG4 mAb with V-regions gLa and gHd is referred to as g5/44.

Identification of CD22 epitope recognized by g5/44

The ability of humanized anti-CD22 mAb, g5/44, to inhibit the binding of various murine anti-CD22 mAbs to CD22 was evaluated by biosensor analysis using a BIA-core (Fig. 7). Many of these murine mAbs have been characterized with respect to their binding to defined epitopes on the extracellular domain of human CD22 [33–36]. As expected, g5/44 binding to CD22-mFc blocked subsequent binding of m5/44. In addition, binding of two other anti-CD22 mAbs—HD239 and S-HCL1/anti-Leu14 (recognizing epitope A located in the first Ig-like domain of CD22) [34, 35]—was also inhibited by g5/44 bound to CD22-mFc. In contrast, three other anti-CD22 mAbs—RFB4 (recognizing epitope B located on the third Ig-like domain of CD22), 4KB128 (recognizing the second Ig-like domain of CD22), and To15 (recognizing epitope C on the fourth Ig-like domain of CD22) [34, 35]—were still able to bind to CD22-mFc in the presence of g5/44. Prior binding of g5/44 to CD22-mFc also inhibited the subsequent binding of anti-CD22 mAbs, SJ10.1H11, MYG13, and m6/13. These results suggest that g5/44 and its murine counterpart, m5/44, both rec-

Anti-CD22 mAb	Epitope	CD22 Ig domain	% Inhibition
HD239	A	1	
SHCL1	A	1	
RFB4	B	3	
To15	C	4	
4KB128	?	2	
m5/44	?	?	
m6/13	?	?	
SJ10	?	?	
MYG13	?	?	

Fig. 7 Effect of humanized anti-CD22 mAb g5/44 on the binding of various murine anti-CD22 mAbs to human CD22-mFc detected by biosensor analysis. Various murine anti-CD22 mAbs were individually (50 µg/ml) allowed to bind CD22-mFc immobilized on biosensor chip that had been pretreated (100 µg/ml) with either anti-CD22 mAb g5/44 or anti-CD33 mAb hP67.6 (control mAb). Percentage Inhibition of murine mAb binding was calculated as $100 \times [1 - (RU \text{ with } g5/44 \text{ pretreatment}) / (RU \text{ with } hP67.6 \text{ pretreatment})]$
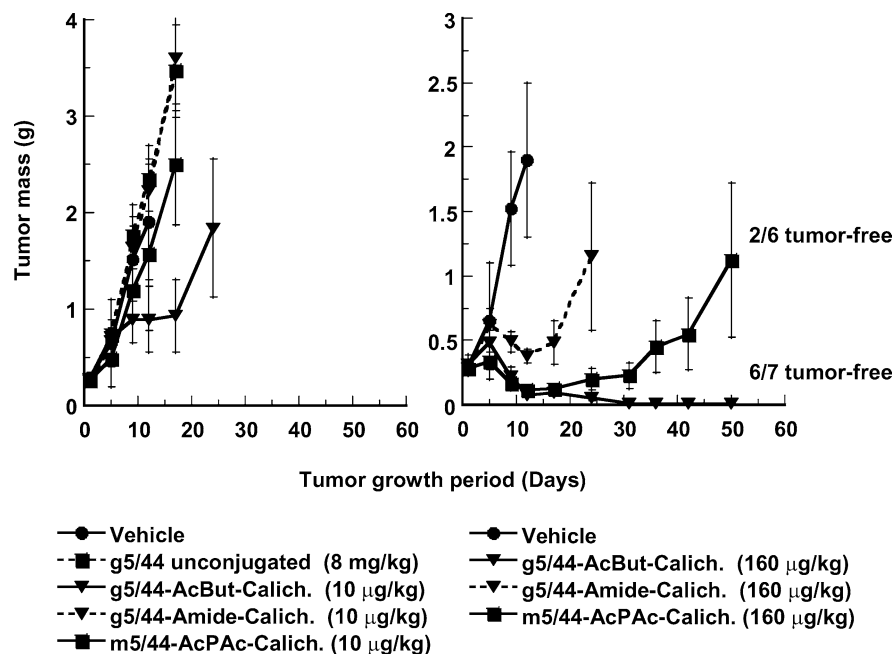
ognize epitope A located in the first N-terminal domain of CD22. The CD22 domain(s) reactive with anti-CD22 mAbs MYG13 and SJ10.1H11 was unknown. However, their blocking by g5/44 suggests that these mAbs also recognize the first Ig-like domain of CD22.

Antitumor activity of calicheamicin conjugated to humanized anti-CD22 mAb g5/44

Humanized anti-CD22 mAb g5/44 was conjugated to CalichDM using either the Amide or the AcBut linker.

Incubation of Ramos BCLs in vitro with CalichDM conjugated to g5/44 via either acid-labile or acid-stable linkers inhibited their growth in vitro with potency similar to that observed with its murine counterparts (data not shown). The ability of CalichDM derivatives conjugated to either m5/44 or g5/44 to inhibit the growth of Ramos BCL xenografts was examined using both the acid-labile (AcPAc for m5/44 and AcBut for g5/44) and the acid-stable (Amide) linker-bearing conjugates. When administered i.p., Q4Dx3 at a dose of 160 µg of conjugated CalichDM/kg, each of the above conjugates caused significant inhibition ($p < 0.05$) of the growth of Ramos BCL xenografts (Fig. 8). At this dose, CalichDMH conjugated to g5/44 via the AcBut linker caused greater and longer lasting inhibition of Ramos BCL growth (85% of mice being tumor-free after 50 days) than the conjugate of m5/44 prepared with the AcPAc linker (28% of tumor-bearing mice being tumor-free after 50 days) ($p < 0.05$ on day 50). In experiments not shown here, the AcBut-linked conjugate of g5/44 often caused long-term regression of established BCL

Fig. 8 Effect of calicheamicin conjugates of murine and humanized anti-CD22 mAbs. Subcutaneous BCLs were established prior to the i.p. administration of CalichDM conjugates at either 10 or 160 µg of conjugated CalichDM/kg. Three such doses were administered 4 days apart (Q4D×3). Unconjugated humanized anti-CD22 mAb, g5/44, was administered i.p. at 8 mg/kg Q4D×3 as a control. Results from a representative experiment are presented as mean tumor mass (g) ± SEM. The number of tumor-free mice is indicated wherever appropriate

2/6 tumor-free

6/7 tumor-free

Tumor growth period (Days)

- ●— Vehicle
- --■-- g5/44 unconjugated (8 mg/kg)
- —▼— g5/44-AcBut-Calich. (10 µg/kg)
- --▽-- g5/44-Amide-Calich. (10 µg/kg)
- —■— m5/44-AcPAc-Calich. (10 µg/kg)

- ●— Vehicle
- —▼— g5/44-AcBut-Calich. (160 µg/kg)
- --▽-- g5/44-Amide-Calich. (160 µg/kg)
- —■— m5/44-AcPAc-Calich. (160 µg/kg)

xenografts without any evidence of re-growth of the tumors for up to 125 days. Among mice treated with a lower dose of conjugated CalichDM (10 µg/kg Q4Dx3), only mice treated with the AcBut-linked conjugate of g5/44 demonstrated significantly smaller tumor masses compared with those in the vehicle-treated mice ($p < 0.05$). The degree of inhibition of BCL growth with the acid-labile AcBut conjugate of g5/44 was greater than that with its acid-stable Amide conjugate ($p < 0.05$ on day 25). The treatment with unconjugated g5/44 (8 mg/kg) had no effect on the growth of Ramos BCL. Together, these results provide convincing evidence of antitumor activity of CD22-targeted conjugates of CalichDM derivatives against human BCL xenografts.

Discussion

Tumor-targeted delivery of calicheamicin, as a conjugate of a mAb reactive against an internalizable TAA, is now a clinically validated therapeutic strategy exemplified by gemtuzumab ozogamicin [5–7]. CD33, the target of gemtuzumab ozogamicin, is a myeloid lineage–specific antigen and is expressed on the vast majority of myeloid malignancies. In order to apply similar antibody-targeted calicheamicin therapy to B-lymphoid malignancies, we focused on the CD22 molecule. CD22 is expressed on the surface of mature B lymphocytes and their malignant counterparts but not their precursors and is known to be internalized upon binding to anti-CD22 mAb [18, 19]. Based on its efficient internalization, CD22 has been the focus of intense investigations for the targeted delivery of immunotoxins and radioimmunotherapy [20–22, 37].

Consistent with the ability of CD22 to facilitate targeted delivery of cytotoxic agents, we have recently described the preclinical antitumor activity of a CD22-targeted immunoconjugate of calicheamicin, CMC-544 [38]. This immunoconjugate comprises a humanized anti-CD22 antibody, g5/44, conjugated to CalichDMH via the AcBut linker [38]. The present study serves as a prelude to the above study describing CMC-544 and represents the evolution of various studies beginning with the selection of murine antibody against human CD22, its ability to modulate cell-surface CD22, its conjugation with calicheamicin, and evidence of the antitumor activity of its calicheamicin conjugates. In addition, the present study also described the humanization of the murine anti-CD22 mAb, epitope mapping of the humanized antibody, g5/44, and, lastly, the evidence of antitumor efficacy of calicheamicin-conjugated humanized anti-CD22 antibody.

To apply a CD22-targeted chemotherapy strategy, a panel of murine anti-human CD22 mAbs were made and evaluated for their affinity of binding to human CD22 on B cells and their ability to cause its internalization. Based on its high-affinity binding to CD22 and also its ability to modulate CD22, mAb m5/44 (murine IgG1) was selected for further studies. CalichDM was conjugated to m5/44 using either the acid-labile AcPAc or acid-stable Amide linker as shown in Fig. 2. The presence of acid-labile hydrazone functionality in the AcBut- or AcPAc-linked conjugates allows, under acidic conditions (pH range of 4.5–6) such as those in the lysosomes, rapid release of CalichDMH from its conjugated state. Binding of the immunoconjugate to the readily internalizable target antigen makes possible efficient intracellular presentation of the conjugated cytotoxic drug.

Some cells may internalize the immunoconjugate by antigen-nonspecific pinocytosis even in the absence of the target antigen. In addition, the immunoconjugates with acid-labile linkage of the drug may release the drug, even in the absence of their internalization, upon acidification of the extracellular environment of metabolically active growing cells. The antibody conjugates with acid-labile linkers that do not bind to the target cells may, therefore, exert some cytotoxic activity in an antigen-nonspecific manner. In contrast, the Amide-linked conjugates may require more extensive "intracellular processing" of the immunoconjugate in order to release the drug. Therefore, in order to be effective, the Amide-linked conjugates of calicheamicin are required to be internalized via specific or nonspecific mechanisms by the target cells. This may explain why the cytotoxic activity of the amide-linked conjugates is often lower than that of AcBut- or AcPAc-linked conjugates as shown in this study.

Both acid-labile and acid-stable conjugates of m5/44 were effective against CD22$^+$ BCLs. The AcPAc-conjugated m5/44 was 4- to 8-fold more potent than the Amide-conjugated m5/44 whose cytotoxic activity was similar to that of unconjugated CalichDMH. Irrespective of the linker used, the CD22-targeted conjugates of calicheamicin were 5- to 30-fold more potent than the nontargeted (antigen-nonspecific) conjugate, CMA-676 bearing the acid-labile AcBut linker. The potent cytotoxic activity of the Amide-linked conjugate of m5/44 is consistent with its efficient internalization by CD22$^+$ BCLs. These results further indicate that the intracellular delivery of CalichDMH resulting from the CD22-mediated internalization of its antibody conjugate followed by the hydrolytic release of CalichDMH is more efficient in inhibiting BCL growth than nontargeted mechanisms of delivery of CalichDMH such as passive diffusion.

Calicheamicin conjugates of m5/44 were also evaluated for their antitumor activity against human Raji and Ramos BCL xenografts in nude mice. Both AcPAc-linked and Amide-linked conjugates of m5/44 were equally effective in inhibiting the tumor growth. In contrast, both unconjugated m5/44 and the CD33-targeted conjugate, CMA-676 (used as a nonbinding control), had no effect on the growth of BCL xenografts. The unconjugated m5/44 was administered at a dose of 8 mg/kg equivalent to the antibody quantity in its calicheamicin conjugates. The antitumor activity of the m5/44 calichDMH conjugates is, therefore, not due to the antibody component of the conjugate. Doses higher than 8 mg/kg

of the unconjugated m5/44 were not administered, so it is not absolutely clear that the naked antibody is completely devoid of antitumor activity. Howerever, the anti-CD22 mAb m5/44 is a murine IgG1 isotype mAb, and the murine IgG1 isotype is unable to fix complement and binds poorly to Fc receptors. Thus, m5/44 would not be expected to mediate ADCC or CDC.

Unconjugated CalichDMH at nonlethal doses had been consistently ineffective in the human tumor xenograft models evaluated so far [39] (E. Boghaert, J. DiJoseph, and C. Discafani, unpublished observations) . In the absence of its tumor-targeting, the poor antitumor activity of CalichDMH is not surprising, and further underscores the therapeutic advantage conferred by the tumor-targeted delivery of cytotoxic agents such as calicheamicin. m5/44 was also evaluated for binding to cryopreserved B-NHL tumor biopsy samples. All of the B-cell NHL samples tested ($n = 50$), including high-grade diffused, mantle cell and follicular NHL, reacted positively with m5/44 (J. Crocker, Birmingham Heartlands Hospital, Birmingham, UK, unpublished observations). This demonstration of m5/44 binding to B-NHL biopsy samples supports its use as a vehicle for targeted delivery of cytotoxic agents such as calicheamicin to CD22$^+$ tumor cells. Based on its binding to B-NHL biopsy samples and potent anti-BCL activity of its conjugate of calicheamicin, m5/44 was selected for preclinical development.

To reduce or eliminate its immunogenicity in humans, the murine m5/44 antibody was humanized by CDR grafting [40]. Variable region heavy and light chain sequences of murine mAb m5/44 exhibited highest homology to human subgroup I of V_H and subgroups I and II of $V\kappa$. Hence, the germline frameworks of human V_H subgroup I (DP7) and human $V\kappa$ subgroup I (DPK9) were selected, and murine CDRs were grafted on the human frameworks. For both heavy and light chain, framework 4 acceptor sequences were derived from human J-region sequences JH-4 and JK-1, respectively. Six distinct grafts were expressed and shown to be equivalent to the original anti-CD22 mAb m5/44 in terms of affinity and competition for binding to CD22 on B cells. In addition, a potential N-linked glycosylation site and a lysine residue in the V_H CDR2 (a potential target for calicheamicin conjugation) were removed to avoid potential interference during binding to CD22.

One such graft, gLb-gHd, was selected to assemble a full antibody with the human IgG4 constant region. This humanized anti-CD22 mAb was referred to as g5/44. The heavy chain amino acid sequences of g5/44 are 91% identical to that of hP67.6, the humanized IgG4 anti-CD33-targeting agent in gemtuzumab ozogamicin. Even if the targeting mAb is humanized, the presence of drug-linker in the mAb conjugate may induce Ab response in patients against the CalichDMH AcBut linker portion of the molecule. However, it is reassuring that no antibodies targeted to either CalichDMH, AcBut linker, or the entire immunoconjugate were detected in 142 patients who received gemtuzumab ozogamicin in a phase

II study [5]. The choice of the human IgG4 constant region in g5/44 was also based on its poor effector capabilities (ADCC and CDC) [41, 42], and hence, the therapeutic effect observed with its conjugate of calicheamicin can be attributed entirely to the targeted delivery to, and subsequent cytotoxicity of, calicheamicin against tumor cells.

Various murine anti-CD22 mAbs have been used to define distinct epitopes located on the Ig-like domains within the extracellular region of human CD22 [34, 35]. Blocking studies using various murine mAbs revealed that humanized anti-CD22 mAb g5/44 inhibits the binding of only those murine anti-CD22 mAbs that had previously been mapped to bind to the first N-terminal Ig-like (IgV) domain of human CD22 [34, 35]. This suggests that g5/44 and its murine counterpart, m5/44, both recognize epitope A located in the N-terminal IgV domain of CD22. Epratuzumab, a humanized IgG1 anti-CD22 mAb (hLL2), is presently being evaluated as a naked antibody therapeutic [43] and also as a CD22-targeted radioimmunotherapeutic agent for the treatment of B-NHL [37]. This mAb has been shown to bind epitope B on human CD22, originally identified by the binding of a murine anti-CD22 mAb, RFB4 [36]. Thus, g5/44 and epratuzumab appear to recognize distinct epitopes on CD22.

Our primary objective with g5/44 is to use it as a CD22-targeted calicheamicin-delivery agent in the treatment of B-lymphoid malignancies, and we have shown here a potent antitumor activity of CalichDMH conjugated to g5/44 against BCL xenografts. We have no evidence to support other potential mechanisms of action, as g5/44 has a human IgG4 isotype and does not demonstrate any ADCC or CDC activity in vitro using a human source of complement and peripheral blood mononuclear cells as effector cells (L. Kalyandrug, unpublished observation) or antitumor effect in vivo ([38] and this study). Some anti-CD22 antibodies have, however, been shown to mediate apoptosis and growth inhibition of BCLs. The N-terminal IgV domain of CD22 is known to bind the natural ligand of CD22, α-2,6-linked sialic acid termini on glycosylated cell-surface structures. Some but not all mAbs reactive with the N-terminal IgV of CD22 have been shown to block the ligand binding by CD22 [34]. One such mAb, HD22-7, caused apoptosis and inhibited the growth of BCL xenografts in nude mice [44]. Whether g5/44 (or m5/44) can inhibit ligand binding by CD22 has not been determined. However, if the ability of an anti-CD22 mAb to cause BCL apoptosis [44] is closely tied with its ability to block ligand binding by CD22 [34], then g5/44 is not expected to be a blocking antibody capable of neutralizing the CD22/ligand interaction.

Our antibody-targeted chemotherapy strategy derives its advantages from the cytotoxic potency of calichDM, high-affinity binding of the targeting antibody conjugate to the targeted TAA, and the antibody-conferred long half-life of the conjugated drug in circulation. Antitumor activity of the mAb-CalichDMH conjugate is

independent of the effector functional capabilities of the targeting antibody. The demonstration of the potent antitumor activity of the calicheamicin conjugates of g5/44 supports its evaluation as a CD22-targeted calicheamicin therapeutic agent in the treatment of B-NHL and other B-lymphoid malignancies. Based on its superior antitumor efficacy, an AcBut-linked conjugate of g5/44 and CalichDMH, designated as CMC-544 [38], has been selected for further development. CMC-544, also known as inotuzumab ozogamicin, is currently being evaluated in phase I clinical trials in B-NHL.

References

1. Trail P, Bianchi A (1999) Monoclonal antibody drug conjugates in the treatment of cancer. Curr Opin Immunol 11:584
2. Dubowchik G, Walker M (1999) Receptor-mediated and enzyme-dependent targeting of cytotoxic anti-cancer drugs. Pharmacol Ther 83:67
3. Damle NK, Frost P (2003) Antibody-targeted chemotherapy with immunoconjugates of calicheamicin. Curr Opin Pharmacol 3:386
4. Bross PF, Beitz J, Chen G, Chen XH, Duffy E, Kieffer L, Roy S, Sridhara R, Rahman A, Willaims G, Pazdur R (2001) Gemtuzumab ozogamicin: approval summary: gemtuzumab ozogamicin in relapsed acute myeloid leukemia. Clin Cancer Res 7:1490
5. Sievers E, Larson R, Stadmauer E, Estey E, Lowenberg BH, Dombret HC, Karanes C, Theobald M, Bennett JM, Sherman ML, Berger MA, Eten CB, Loken MR, van Dongen JJM, Bernstein ID, Appelbaum FR (2001) Efficacy and safety of gemtuzumab ozogamicin in patients with CD33-positive acute myeloid leukemia in first relapse. J Clin Oncol 19:3244
6. Larson R, Boogaerts M, Estey E, Karanes C, Stadtmauer EA, Sievers EL, Mineur P, Bennett JM, Berger MS, Eten CB, Muntean M, Loken MR, van Dongen JJM, Bernstein ID, Applebaum FR (2002) Antibody-targeted chemotherapy of older patients with acute myeloid leukemia in first relapse using Mylotarg (gemtuzumab ozogamicin). Leukemia 16:1627
7. Berger M, Leopold L, Dowell J, Korth-Bradley J, Sherman M (2002) Licensure of gemtuzumab ozogamicin for the treatment of selected patients 60 years of age or older with acute myeloid leukemia in first relapse. Invest New Drugs 20:395
8. Hamann P, Hinman L, Beyer C, Lindh D, Upeslacis J, Flowers DA, Bernstein I (2002) An anti-CD33 antibody-calicheamicin conjugate for treatment of acute myeloid leukemia: choice of linker. Bioconjug Chem 3:40
9. Hamann P, Hinman L, Hollander I, Beyer CF, Lindh D, Holcomb R, Hallett W, Tsou HR, Upeslacis J, Schohat D, Mountain A, Flowers DA, Bernstein I (2002) Gemtuzumab ozogamicin, a potent and selective anti-CD33 antibody-calicheamicin conjugate for treatment of acute myeloid leukemia. Bioconjug Chem 13:47
10. Zein N, Sinha A, McGahren W, Ellestad G (1988) Calicheamicin γI: an antitumor antibiotic that cleaves double-stranded DNA site specifically. Science 240:1198
11. Lee MD, Dunne TS, Chang CC, Siegel MM, Morton GO, Ellestad GA, McGahren WJ, Borders DB (1992) Calicheamicins, a novel family of antibiotics, 4: Structural elucidations of calicheamicins. J Am Chem Soc 114:985
12. Thorson J, Sievers E, Ahlert J, Shepard E, Whitwam RE, Onwueme KC, Ruppen M (2000) Understanding and exploiting nature's chemical arsenal: the past, present and future of calicheamicin research. Curr Pharm Des 6:1841
13. Mylotarg label. http://www.fda.gov/cder/foi/label/2000/21174lbl.pdf
14. Moyron-Quiroz JE, Partida-Sanchez S, Donis-Hernandez R, Sandoval-Montes C, Santos-Argumedo L (2002) Expression and function of CD22, a B-cell restricted molecule. Scand J Immunol 55:343
15. Tedder TF, Tuscano J, Sato S, Kehrl JH (1997) CD22, a B lymphocyte-specific adhesion molecule that regulates antigen receptor signaling. Ann Rev Immunol 15:481
16. Crocker PR, Varki A (2001) Siglecs, sialic acids and innate immunity. Trends Immunol 22:337
17. Nitschke L, Floyd H, Crocker PR (2001) New functions for the sialic acid-binding adhesion molecule CD22, a member of the growing family of Siglecs. Scand J Immunol 53:227
18. Hanna R, Ong GL, Mattes MJ (1996) Processing of antibodies bound to B-cell lymphomas and other hematological malignancies. Cancer Res 56:3062
19. Shan D, Press OW (1995) Constitutive endocytosis and degradation of CD22 by human B cells. J Immunol 154:4466
20. Kreitman RJ, Wilson WH, Bergeron K, Raggio M, Stetler-Stevenson M, Fitzgerald DJ, Pastan I (2001) Efficacy of the anti-CD22 recombinant immunotoxin BL22 in chemotherapy-resistant hairy-cell leukemia. N Engl J Med 345:241
21. Pastan I, Kreitman RJ (2002) Immunotoxins in cancer therapy. Curr Opin Investig Drugs 3:1089
22. Hursey M, Newton DL, Hansen HJ, Ruby D, Goldenberg DM, Rybak SM (2002) Specifically targeting the CD22 receptor of human B-cell lymphomas with RNA damaging agents: a new generation of therapeutics. Leuk Lymphoma 43:953
23. Galfrè G, Howe SC, Milstein C (1977) Antibodies to major histocompatibility antigens produced by hybrid cell lines. Nature 266:550
24. Morgan A, Jones ND, Nesbitt AM, Chaplin L, Bodmer MW, Emtage JS (1995) The N-terminal end of the CH2 domain of chimeric human IgG1 anti-HLA-DR is necessary for C1q, Fc gamma RI and Fc gamma RIII binding. Immunology 86:319
25. Hinman LM, Hamann PR, Wallace R, Menendez AT, Dur FE, Upeslacis J (1993) Preparation and characterization of monoclonal antibody conjugates of the calicheamicins: a novel and potent family of antitumor antibiotics. Cancer Res 53:3336
26. Coligan JE, Cruisbeek AM, Margulies DH, Shevach EM, Strober W (eds) (1992) Current protocols in immunology, vol 2. Wiley, New York
27. Adair JR, Athwal DS, Emtage JS (1991) Humanised antibodies. International Patent Publication WO91/09967
28. Owens RJ, Young RJ (1994) The genetic engineering of monoclonal antibodies. J Immunol Methods 168:149
29. Tomlinson IM, Walter G, Marks JD, Llewelyn MB, Winter G (1992) The repertoire of human germline VH segments reveals about fifty groups of VH segments with different hypervariable loops. J Mol Biol 227:776
30. Cox JPL, Tomlinson IM, Winter G (1994) A directory of human germ-line V kappa segments reveals a strong bias in their usage. Eur J Immunol 24:827
31. Kabat EA, Wu TT, Perry HM, Gottesman KS, Foeller C (1991) Sequences of proteins of immunological interest, 5th edn. Public Health Service, National Institutes of Health, Bethesda, MD
32. Chothia C, Lesk AM, Tramontano A, Levitt M, Smith-Gill J, Air G, Sheriff S, Padlan EA, Davies D, Tulip WR, Colman PM, Spinelli S, Alzari PM, Poljak RJ (1989) Conformations of immunological hypervariable regions. Nature 342:877
33. Li JL, Shen GL, Ghetie MA, May RD, Till M, Ghetie V, Uhr JW, Janossy G, Thorpe PE, Amlot P (1989) The epitope specificity and tissue reactivity of four murine monoclonal anti-CD22 antibodies. Cell Immunol 118:85

34. Engel P, Wagner N, Miller AS, Tedder TF (1995) Identification of the ligand-binding domains of CD22, a member of the immunoglobulin superfamily that uniquely binds a sialic acid-dependent ligand. J Exp Med 181:1581

35. Engel P, Wagner N, Smith H, Tedder TF (1995) Structure/function analysis of CD22: domains that mediate adhesion. In: Leukocyte typing V. Oxford University Press, Oxford, pp 526–527

36. Stein R, Belisle E, Hansen HJ, Goldenberg DM (1993) Epitope specificity of the anti-(B cell lymphoma) monoclonal antibody, LL2. Cancer Immunol Immunother 37:293

37. Griffiths GL, Govindan SV, Sharkey RM, Fisher DR, Goldenberg DM (2003) [90] Y-DOTA-hLL2: an agent for radioimmunotherapy of non-Hodgkin's lymphoma. J Nucl Med 44:77

38. DiJoseph JF, Armellino DC, Boghaert E, Khandke K, Dougher Sridharan L, Kunz A, Hamann PR, Gorovits B, Udata C, Moran JK, PopplewelL AG, Stephens S, Frost P, Damle NK (2004) Antibody-targeted chemotherapy with CMC-544: a CD22-targeted immunoconjugate of calicheamicin for the treatment of B lymphoid malignancies. Blood 103:1807

39. Hinman LM, Hamann PR, Upeslacis J (1995) Preparation of conjugates to monoclonal antibodies. In: Borders DB, Doyle TW (eds) Endiyne antibiotics as antitumor agents. Dekker, New York, pp 87–106

40. Co MS, Queen C (1991) Humanized antibodies for therapy. Nature 351:501

41. Burton DR, Woof JM (1992) Human antibody effector function. Adv Immunol 51:1

42. Greenwood J, Clark M, Waldmann H (1993) Structural motifs involved in human IgG antibody effector functions. Eur J Immunol 5:1098

43. Leonard JP, Coleman M, Ketas JC, Chadburn A, Ely S, Furman RR, Wegener WA, Hansen HJ, Ziccardi H, Eschenberg M, Gayko U, Cessano A, Goldenberg DM (2003) Phase I/II trial of epratuzumab (humanized anti-CD22 antibody) in indolent non-Hodgkin's lymphoma. J Clin Oncol 21:3051

44. Tuscano JM, O'Donnell RT, Miers LA, Kroger LA, Kukis DL, Lambom KA, Tedder TF, DeNardo GL (2003) Anti-CD22 ligand-blocking antibody HB22.7 has independent lymphomacidal properties and augments the efficacy of [90] Y-DOTA-peptide-Lym-1 in lymphoma xenografts. Blood 101:3641